Available online at www.sciencedirect.com
ScienceDirect
Surface Science 602 (2008) L29–L32
SURFACE SCIENCE
www.elsevier.com/locate/susc

Surface Science Letters

Scanning tunneling microscopy imaging of facet surfaces of self-organized nanocrystal using metal-coated carbon nanotube tip

Yuya Murata, Takehiko Kimura, Takashi Matsumoto, Shin-ichi Honda, Mitsuhiro Katayama *

Division of Electrical, Electronic and Information Engineering, Graduate School of Engineering, Osaka University, 2-1 Yamadaoka, Suita, Osaka 565-0871, Japan

Received 23 October 2007; accepted for publication 29 December 2007
Available online 9 January 2008

Abstract

The facet surfaces of a self-organized $ErSi_2$ nanocrystal were observed by the STM with a metal-coated carbon nanotube tip. The 10-nm-scale radius and high aspect ratio of the tip was able to provide detailed images of the facet surfaces. The stereographic STM imaging showed that the nanocrystal had (1 0 5) facets of the tetragonal $ErSi_2$ on all facet surfaces with a 1×1 periodicity. Bias-dependent STM images revealed that the facet surface has a bulk-truncated structure consisting of Si dimers and Er atoms. Moreover, scanning tunneling spectroscopy exhibited a difference in density of states between top and facet surfaces.

Keywords: Scanning tunneling microscopy; Carbon nanotube tip; Erbium silicide; Nanocrystal

Self-organized nanocrystals on a Si surface have attracted considerable interest from the standpoint of both device application and fundamental science. To clarify their formation mechanism and open opportunities in device application, it is essential to elucidate their surface structures and electronic properties. In studies of Ge nanocrystals on Si, the topography of nanocrystals and their evolution in size and shape were extensively investigated by various methods such as atomic force microscopy [1], transmission electron microscopy (TEM) [2], low-energy electron microscopy [3], and grazing incidence small angle X-ray scattering [4]. On the other hand, scanning tunneling microscopy (STM) studies [5–7] yielded the surface periodic structures of the Ge/Si(1 0 0) nanocrystal including the {1 0 5} facet, which is tilted by a slope angle of 11.3° from the substrate plane. However, the steeper the slope angle of facet surfaces, the more difficult in observation of the surface structure of the facets. This is because a conventional metal tip has a radius of approximately 100 nm and conical shape, which prevents easy access to the steep facet surface.

Carbon nanotubes (CNTs) have been regarded as an ideal nanomaterial of the STM tip apex due to their superior properties such as nanometer-scale radius, high aspect ratio, and mechanical robustness. We have recently developed a high-yield fabrication process for CNT tips coated with a thin PtIr layer to stabilize their overall conductivity [8]. The geometrical and electrical advantages of the PtIr-coated CNT tip were demonstrated in single- and multi-probe STM [9,10].

In this study, we used the PtIr-coated CNT tip for the STM imaging of the facet surfaces of an $ErSi_2$ nanocrystal on Si(1 0 0). The atomic-resolution image and the scanning tunneling spectroscopy (STS) measurement showed the surface periodic structure and the electronic density of states specific to the facet surface. Furthermore, a structural model was proposed on the basis of bias-dependent STM results.

The detailed fabrication process for PtIr-coated CNT tips has been described elsewhere [8]. From scanning

* Corresponding author. Tel.: +81 6 6879 7775; fax: +81 6 6876 4564.
E-mail address: katayama@nmc.eei.eng.osaka-u.ac.jp (M. Katayama).

0039-6028/$ - see front matter © 2008 Elsevier B.V. All rights reserved.
doi:10.1016/j.susc.2007.12.039

electron microscopy (SEM) and TEM observations, it was confirmed that the PtIr-coated CNT had a length of about 200 nm and a radius of curvature of about 10 nm. The PtIr-coated CNT tip and Si(1 0 0) substrate were introduced into an STM chamber with a base pressure of 1×10^{-8} Pa. The Si(1 0 0) substrate was degassed at 900 °C and cleaned above 1150 °C by direct current heating. Er was deposited onto the substrate at room temperature, and the sample was subsequently annealed at 900 °C for 10 min, and then cooled down to room temperature. We repeated this sequence several times, and obtained silicide islands with a height of several tens of nm. Then, STM observations were carried out at room temperature. After STM observations, the sample was *ex situ* characterized by TEM.

From the STM imaging of several $ErSi_2$ islands, the islands were found to have a rectangular base with sides parallel to $\langle 1\,1\,0\rangle_{Si}$ directions, a width of 50–200 nm and a height of 20–50 nm, similar to the AFM study reported by Peto et al. [11]. Fig. 1a shows a typical STM image of an $ErSi_2$ nanocrystal obtained using the PtIr-coated CNT tip. Four flat facet surfaces were clearly observed around the top surface. Line profiles in Fig. 1b and c show that each of the four facets formed a slope angle of about 34° with respect to the substrate plane. On the other hand, when we used the conventional W tip with a typical radius of curvature of 100 nm for STM imaging, a blunt and non-uniform structure was observed at the facet surface of the nanocrystal, due to the artifact produced by the conical shape of the tip apex. This indicates that we can reduce the scale of such artifacts to less than 10 nm using the PtIr-coated CNT tip. The PtIr-coated CNT tip also induces some artifacts in the images, but they have nanometer-scale tolerances. Due to the tip radius of 10 nm, the nanocrystal was likely to have a few nm larger width than it really have, and the roundly eroded image emerges around the top edges of the nanocrystal. The area of the bottom edges with a height of a few nm could not be observed.

High-resolution STM images of top and facet surfaces are shown in Fig. 2. The unit mesh of each surface is shown by the solid square. The superstructure of the top surface was identified to be a c(2 × 2) reconstruction with a periodicity of 0.56 nm, consistent with the previous study [12]. Fig. 2b and c shows a three-dimensional image, and a two-dimensional image viewed from the direction normal to the facet surface, taken at the square area on the facet surface in Fig. 1a. From Fig. 2c, it was found that the surface periodic structure on the facet surface has a centered rectangular lattice with a short side parallel to the edge of the nanocrystal, in which the periodicity parallel to the edge was 0.4 nm, and the periodicity up the face of a facet was 2.4 nm. Using the slope angle of 34°, the periodicity in the direction normal to the substrate was estimated to be about 1.3 nm. This length agrees with the lattice constant of 1.326 nm along the *c*-axis in the tetragonal $ThSi_2$-type $ErSi_2$. It was reported that both tetragonal $ThSi_2$-type [12] and hexagonal AlB_2-type [11] crystallites have been found for $ErSi_{2-x}$/Si(1 0 0) epitaxial growth. Their epitaxial relations on Si(1 0 0) are tetragonal $ErSi_2(1\,0\,0)\|Si(1\,0\,0)$ (the *a* and *b* axes are parallel to the surface) and hexagonal $ErSi_2(1\,\bar{1}\,0\,0)\|Si(1\,0\,0)$ (the *a* and *c* axes are parallel to the surface). The isotropic slope angle of each facet surface is

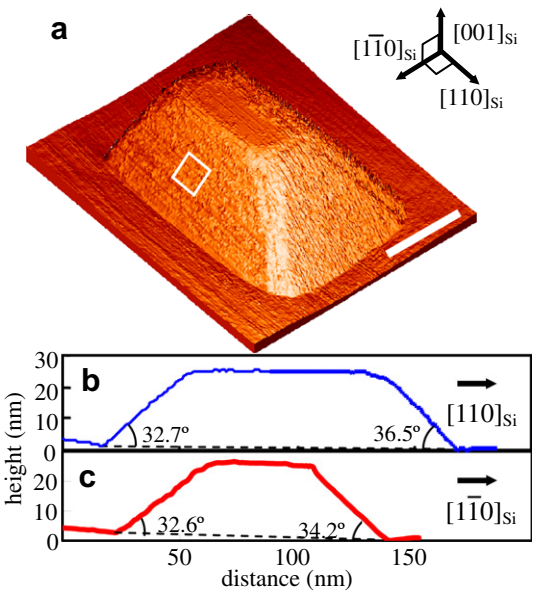

Fig. 1. (a) An STM image of an $ErSi_2$ nanocrystal (scale bar: 50 nm, $V_s = -1.5$ V, $I = 0.4$ nA). (b) and (c) Line profiles along $[1\,1\,0]_{Si}$ and $[1\,\bar{1}\,0]_{Si}$ directions.

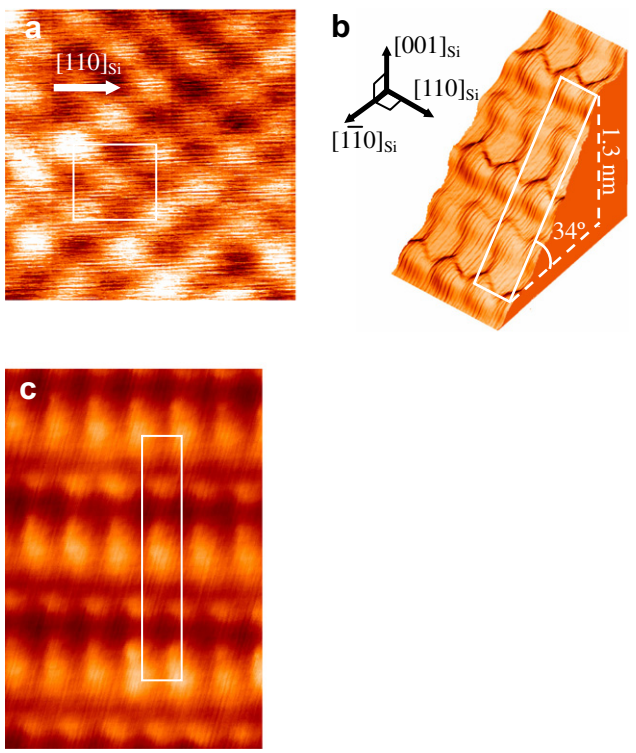

Fig. 2. (a) An STM image of the top surface (3.4 × 3.4 nm^2, $V_s = -0.2$ V, $I = 0.4$ nA). (b) A three-dimensional STM image of the facet surface ($V_s = -0.7$ V, $I = 0.4$ nA). (c) An STM image of the facet surface viewed from the direction normal to the surface (2.6 × 3.7 nm^2, $V_s = -0.7$ V, $I = 0.4$ nA).

reasonable for the formation of the tetragonal $ErSi_2$ crystallite, since the tetragonal $ErSi_2$ has isotropic lattice constants along the two orthogonal $[1\,1\,0]_{Si}$ directions ($a = b =$ 0.396 nm), whereas the hexagonal $ErSi_2$ has anisotropic ones ($a = 0.3785$ nm, $c = 0.408$ nm).

From the slope angle of 34°, all four facet surfaces are determined to be {1 0 5} planes of the tetragonal $ThSi_2$-type $ErSi_2$. This finding was also confirmed by the *ex situ* cross-sectional TEM observation (not shown) after STM observation. Additionally, the detailed inspection of the STM image showed that the unit mesh of the facet surface (0.4 nm × 2.4 nm) corresponded to the 1 × 1 periodicity in the $ThSi_2$-type $ErSi_2$(1 0 5) plane (0.396 nm × 2.383 nm).

Fig. 3a shows a dual-polarity STM image of the facet surface together with a schematic showing the positions of maxima. This is a projected image onto the substrate plane. The right side of the image is closer to the top of the nanocrystal than the left side. STM maxima were composed of bias-independent brighter rows, and bias-dependent darker ovals between brighter rows. In the empty state, darker ovals appeared right in the middle of brighter rows, while in the filled state, the positions of these ovals were shifted by 0.24 nm toward the top of the nanocrystal. A similar dependence on bias polarity was seen in the voltage range from +2.0 V to −2.0 V.

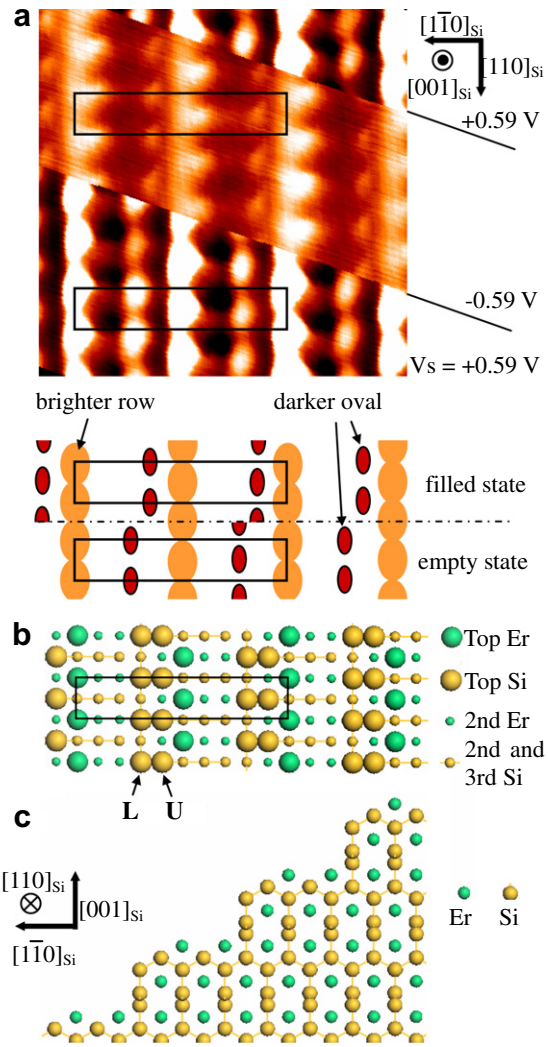

Fig. 3. (a) A dual-polarity STM image of the facet surface with schematic highlighting maxima (3.4×3.4 nm^2, $V_s = \pm 0.6$ V, $I = 0.4$ nA). (b) The proposed model of the facet surface viewed from the direction normal to the substrate plane. The topmost Er and Si atoms are illustrated as larger spheres. (c) A side view of the proposed model.

On the basis of the STM results, we proposed a structural model for the facet surface. A proposed model is shown from the view of the direction normal to the substrate plane in Fig. 3b, and from the side view in Fig. 3c. Since the 1 × 1 periodicity was preserved on this surface, the surface reconstruction over a unit mesh is not likely to occur. There are some cleavage surfaces when one cleaves the $ErSi_2$ crystal along the {1 0 5} plane. This proposed model represents one of the as-cleaved surfaces, in which we correlated bias-dependent and -independent maxima in the STM image to the topmost Si dimer and Er atom (illustrated as larger spheres in Fig. 3b), respectively. The bias-dependent changes in the STM image reflect differences in the spatial contribution of occupied and unoccupied states. We interpreted darker ovals in the filled state and those in the empty state as a bonding orbital at the center of the topmost Si dimer and an antibonding orbital of a dangling bond of the lower Si atom in the dimer (labeled L in Fig. 3b), respectively. The dangling bonds of the upper Si atoms (labeled U) were expected to represent protrusions in the empty state, however, they were not clearly observed. It is likely that the buckling of the Si dimers occurred due to charge transfer from the lower Si atoms to the upper ones, so that only the lower Si atoms contributed to the empty state image. Consequently, it was suggested that maxima in bias-independent brighter rows correspond to the positions of Er atoms. It can be ruled out that the charge transfer between Si and Er atoms [13] might bring STM maxima in the empty and filled states that emerge at surface Si and Er atoms, since there were bias-independent brighter rows.

The electronic property of the nanocrystal was measured by STS. Fig. 4 shows STS spectra of the top and facet surfaces. Each spectrum was an averaged one of several hundreds of *I–V* curves taken at unspecified sites on each surface. The spectrum obtained at the top surface exhibited the finite density of states (DOS) near the Fermi level, which was consistent with the report that the tetragonal

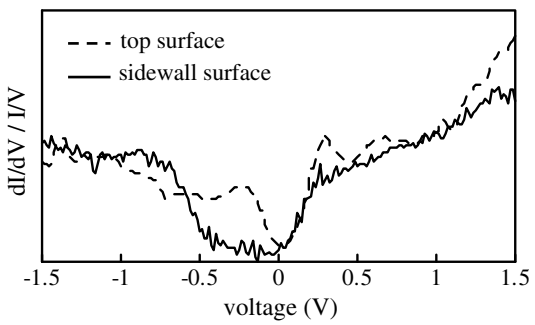

Fig. 4. STS spectra of the top and facet surfaces.

$ErSi_2$ film had a metallic property [14]. On the other hand, the DOS close below the Fermi level was evidently reduced in the spectrum at the facet surface, which was likely to exhibit a semimetallic behavior. However, the origin of the difference in the DOS between the two surfaces was not elucidated yet. In the near future, the theoretical investigations combined with site-specific STS measurements will uncover the mechanism of the emergence of the peculiar electronic state of the facet surface observed in this study.

In conclusion, we have investigated the surface structure and density of states of the facet surface of an $ErSi_2$ nanocrystal using a PtIr-coated CNT tip. Stereographic STM imaging revealed that the facet surface has a bulk-truncated structure of tetragonal $ErSi_2(1\,0\,5)$, which consists of Si dimers and Er atoms. The STS spectra showed difference in density of states close below the Fermi level between the facet and the top surface. Our method presented in this study will provide a novel route to the atomic-scale investigation of the structure and the density of states of three-dimensional nanostructures.

Acknowledgements

This work was supported in part by the SENTAN program of the Japan Science and Technology Agency and by a Grant-in-Aid for Scientific Research from the Japan Society for the Promotion of Science. One of the authors (Y.M.) acknowledges support from the Japan Society for the Promotion of Science.

References

[1] F. Boscherini, G. Capellini, L. Di Gaspare, M. De Seta, F. Rosei, A. Sgarlata, N. Motta, S. Mobilio, Thin Solid Films 380 (2000) 173.
[2] C. Lang, S. Kodambaka, F.M. Ross, D.J.H. Cockayne, Phys. Rev. Lett. 97 (2006) 226104.
[3] F.M. Ross, R.M. Tromp, M.C. Reuter, Science 286 (1999) 1931.
[4] M.-I. Richard, T.-U. Shulli, E. Wintersberger, G. Renaud, G. Bauer, Nucl. Instrum. Methods Phys. Res., Sect. B 246 (2006) 35.
[5] T. Eguchi, Y. Fujikawa, K. Akiyama, T. An, M. Ono, T. Hashimoto, Y. Morikawa, K. Terakura, T. Sakurai, M.G. Lagally, Y. Hasegawa, Phys. Rev. Lett. 93 (2004) 266102.
[6] M. Tomitori, K. Watanabe, M. Kobayashi, F. Iwawaki, O. Nishikawa, Surf. Sci. 301 (1994) 214.
[7] Y.-W. Mo, D.E. Savage, B.S. Swartzentruber, M.G. Lagally, Phys. Rev. Lett. 65 (1990) 1020.
[8] H. Konishi, Y. Murata, W. Wongwiriyapan, M. Kishida, K. Tomita, K. Motoyoshi, S. Honda, M. Katayama, S. Yoshimoto, K. Kubo, R. Hobara, I. Matsuda, S. Hasegawa, M. Yoshimura, J.-G. Lee, H. Mori, Rev. Sci. Instrum. 78 (2007) 013703.
[9] T. Ikuno, M. Katayama, M. Kishida, K. Kamada, Y. Murata, T. Yasuda, S. Honda, J.-G. Lee, H. Mori, K. Oura, Jpn. J. Appl. Phys. 43 (2004) L644.
[10] S. Yoshimoto, Y. Murata, K. Kubo, K. Tomita, K. Motoyoshi, T. Kimura, H. Okino, R. Hobara, I. Matsuda, S. Honda, M. Katayama, S. Hasegawa, Nano Lett. 7 (2007) 956.
[11] G. Peto, G. Molnar, Z.E. Horvath, Cs.S. Daroczi, E. Zsoldos, J. Gyulai, Surf. Sci. 578 (2005) 142.
[12] G. Chen, J. Wan, J. Yang, X. Ding, L. Ye, X. Wang, Surf. Sci. 513 (2002) 203.
[13] J.Y. Veuillen, T.A.N. Tan, D.B.B. Lollman, N. Guerfi, R. Cinti, Surf. Sci. 251/252 (1991) 432.
[14] D. Tsamakis, M. Vlachos, A. Travlos, N. Salamouras, Thin Solid Films 418 (2002) 211.